Struct Multidisc Optim (2010) 40:53–64
DOI 10.1007/s00158-009-0359-3

RESEARCH PAPER

Topological derivative for steady-state orthotropic heat diffusion problem

S. M. Giusti · A. A. Novotny · J. Sokołowski

Received: 14 October 2008 / Revised: 8 January 2009 / Accepted: 12 January 2009 / Published online: 7 February 2009

Abstract The aim of this work is to present the calculation of the topological derivative for the total potential energy associated to the steady-state orthotropic heat diffusion problem, when a circular inclusion is introduced at an arbitrary point of the domain. By a simple change of variables and using the first order Pólya-Szegö polarization tensor, we obtain a closed formula for the topological sensitivity. For the sake of completeness, the analytical expression for the topological derivative is checked numerically using the standard Finite Element Method. Finally, we present two numerical experiments showing the influency of the orthotropy in the topological derivative field and also one example concerning the optimal design of a heat conductor.

Keywords Topological asymptotic analysis · Steady-state orthotropic heat diffusion · Topological derivative · Polarization tensor

S. M. Giusti · A. A. Novotny (✉)
Laboratório Nacional de Computação Científica
LNCC/MCT, Av. Getúlio Vargas 333,
25651-075 Petrópolis, Rio de Janeiro, Brasil
e-mail: novotny@lncc.br

J. Sokołowski
Institut Elie Cartan, Laboratoire de Mathématiques,
Université Henri Poincaré Nancy I, B.P. 239,
54506 Vandoeuvre lès Nancy Cedex, France
e-mail: Jan.Sokolowski@iecn.u-nancy.fr

1 Introduction

The topological sensitivity analysis gives the topological asymptotic expansion of a shape functional with respect to an infinitesimal singular domain perturbation, like the insertion of holes, inclusions, source-term or cracks. The main term of this expansion, called topological derivative (Eschenauer et al. 1994; Sokołowski and Żochowski 1999; Céa et al. 2000), is now of common use in numerical procedures of resolution for topology optimization (Amstutz and Andrä 2006; Lee and Kwak 2008), image processing (Hintermüller 2005; Auroux et al. 2007; Larrabide et al. 2008) and inverse problems (Feijóo 2004; Amstutz et al. 2005; Bonnet 2006). Concerning the theoretical development of the topological asymptotic analysis, the reader may refer to Nazarov and Sokołowski (2003), for instance. We refer the reader to Allaire et al. (2005); Norato et al. (2007); Fulmanski et al. (2007) and Fulmanski et al. (2008), for the numerical methods of shape and topology optimization which include the topological derivatives in the numerical procedure of the *levelset* type.

In order to introduce these concepts, let us consider an open bounded domain $\Omega \subset \mathbb{R}^2$, which is submitted to a non-smooth perturbation in a small region $\omega_\varepsilon(\widehat{\mathbf{x}}) = \varepsilon\omega$ of size ε with center at an arbitrary point $\widehat{\mathbf{x}} \in \Omega$. Thus, we assume that a given shape functional ψ admits the following topological asymptotic expansion

$$\psi(\Omega_\varepsilon) = \psi(\Omega) + f(\varepsilon) D_T(\widehat{\mathbf{x}}) + o(f(\varepsilon)) \,, \tag{1}$$

where Ω_ε is the topologically perturbed domain and $f(\varepsilon)$ is a positive function that decreases monotonically such that $f(\varepsilon) \to 0$ when $\varepsilon \to 0$. Then, the term $D_T(\widehat{\mathbf{x}})$

is defined as the topological derivative of ψ. Therefore, this derivative can be seen as a first order correction on $\psi(\Omega)$ to estimate $\psi(\Omega_\varepsilon)$. In addition, from (1), we have that the classical definition of the topological derivative is given by

$$D_T(\widehat{\mathbf{x}}) = \lim_{\varepsilon \to 0} \frac{\psi(\Omega_\varepsilon) - \psi(\Omega)}{f(\varepsilon)} \,. \tag{2}$$

On the other hand, in the work of Sokołowski and Żochowski (1999), the topological sensitivity associated to the nucleation of a hole in a domain characterized by an orthotropic material was calculated. In order to simplify the analysis, the domain was perturbed introducing an elliptical hole oriented in the directions of the orthotropy and with semi-axis proportional to the material properties coefficients in each orthogonal direction. In this paper, we extend the above result considering as perturbation a small circular inclusion of size ε of the same nature as the bulk material (see Fig. 1), instead of an elliptical hole. In summary, we present the calculation of the topological derivative for the total potential energy associated to the steady-state orthotropic heat diffusion problem, considering the nucleation of a small circular inclusion.

This paper is organized as follows. Section 2 describes the model associated to the steady-state orthotropic heat diffusion problem. The topological sensitivity analysis of the total potential energy associated to the problem under consideration is developed in Section 3, where we present the main result of the paper: a closed formula for the topological derivative. In addition, a simple finite element-based numerical example is also provided for the numerical verification of the analytically derived topological derivative formula. In Section 4 are presented two numerical experiments showing the behavior of the topological sensitivity field for different values of the orthotropic thermal conductivities and also one example concerning the optimal design of heat conductors. The paper ends in Section 5 where concluding remarks are presented.

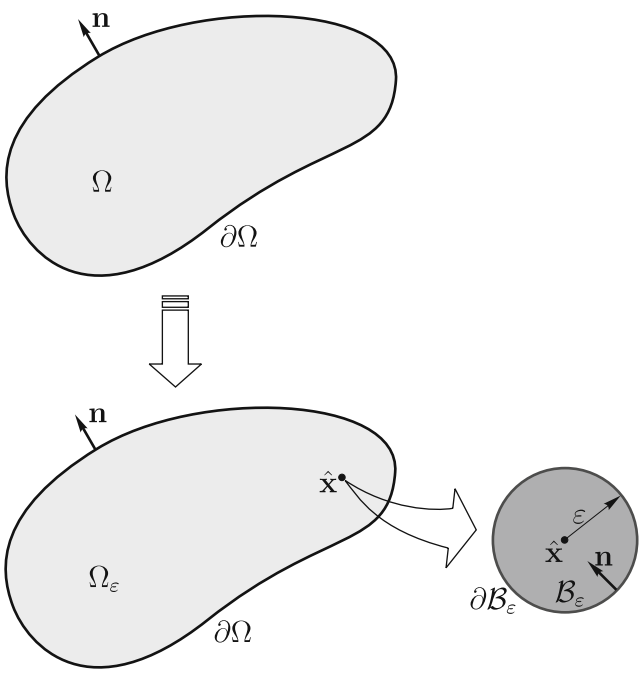

Fig. 1 Topological derivative concept

2 Formulation of the problem

As mentioned in the previous section, the topological asymptotic analysis of the total potential energy associated to the steady-state orthotropic heat diffusion problem is calculated. Thus, the unperturbed shape functional is defined as:

$$\psi(\Omega) := \mathcal{J}_\Omega(u) = \frac{1}{2}\int_\Omega \mathbf{K}\nabla u \cdot \nabla u - \int_\Omega b\,u + \int_{\Gamma_N} \bar{q}u \,, \tag{3}$$

where $\mathbf{K}$ is a symmetric second order thermal conductivity tensor with eigenvalues k_1 and k_2, respectively associated to the orthogonal directions $\mathbf{e}_1$ and $\mathbf{e}_2$, b is a heat source in Ω and u is solution of the following variational problem: find the temperature field $u \in \mathcal{U}(\Omega)$, such that

$$\int_\Omega \mathbf{K}\nabla u \cdot \nabla \eta - \int_\Omega b\,\eta + \int_{\Gamma_N} \bar{q}\eta = 0 \qquad \forall \eta \in \mathcal{V}(\Omega) \,. \tag{4}$$

In the variational problem (4) the set of admissible temperature fields, $\mathcal{U}(\Omega)$, and the space of admissible virtual temperature fields, $\mathcal{V}(\Omega)$, are given by

$$\mathcal{U}(\Omega) := \left\{u \in H^1(\Omega) : u|_{\Gamma_D} = \bar{u}\right\}, \tag{5}$$

$$\mathcal{V}(\Omega) := \left\{\eta \in H^1(\Omega) : \eta|_{\Gamma_D} = 0\right\}. \tag{6}$$

In addition, $\partial\Omega = \Gamma_N \cup \Gamma_D$ with $\Gamma_N \cap \Gamma_D = \varnothing$, where Γ_N and Γ_D are Neumann and Dirichlet boundaries, respectively. Thus, $\bar{u}$ is a Dirichlet data on Γ_D and $\bar{q}$ is a Neumann data on Γ_N, both assumed to be smooth enough, see Fig. 2.

In our particular case, we consider a perturbation on the domain given by the nucleation of a small circular inclusion with thermal conductivity property $\gamma\mathbf{K}$ and heat source δb, where $\mathbf{K}$ is the thermal conductivity and b is the heat source, both associated to the bulk material, and parameters $\gamma \in [0, \infty)$, $\delta \in [-c, c]$ with c

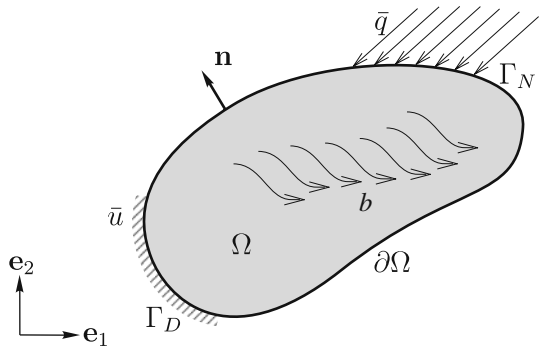

Fig. 2 Formulation of the problem

limited, represent the contrasts in the material property and in the heat source, respectively. We assume that there is a small inclusion $\mathcal{B}_\varepsilon(\hat{\mathbf{x}})$ in the region Ω, which leads to the perturbed domain denoted as Ω_ε. If the inclusion becomes a cavity, it is denoted by $\omega_\varepsilon = \mathcal{B}_\varepsilon(\hat{\mathbf{x}})$. The cavity can be obtained from the inclusion by the limit passage $\gamma \to 0$. In the case of inclusion, the region Ω_ε is decomposed into two disjoint parts $\Omega \setminus \overline{\mathcal{B}_\varepsilon(\hat{\mathbf{x}})}$ and $\mathcal{B}_\varepsilon(\hat{\mathbf{x}})$ with different material properties and heat sources, namely $\mathbf{K}$, $\gamma\mathbf{K}$ and b, δb, respectively. The other limit passage with the contrast $\gamma \to \infty$ results in the ideal thermal conductor inclusion $\omega_\varepsilon = \mathcal{B}_\varepsilon(\hat{\mathbf{x}})$.

Now, tacking into account the definition of the perturbed domain Ω_ε and considering an inclusion of the same nature as the bulk material but with contrasts γ and δ, the perturbed shape functional can be written as:

$$\psi(\Omega_\varepsilon) := \mathcal{J}_{\Omega_\varepsilon}(u_\varepsilon) = \frac{1}{2}\int_{\Omega_\varepsilon} \gamma_\varepsilon \mathbf{K}\nabla u_\varepsilon \cdot \nabla u_\varepsilon - \int_{\Omega_\varepsilon} \delta_\varepsilon b\, u_\varepsilon + \int_{\Gamma_N} \bar{q} u_\varepsilon \,, \tag{7}$$

where parameters γ_ε and δ_ε are defined as

$$\gamma_\varepsilon := \begin{cases} 1 \text{ if } \mathbf{x} \in \Omega \setminus \overline{\mathcal{B}_\varepsilon(\hat{\mathbf{x}})} \\ \gamma \text{ if } \mathbf{x} \in \mathcal{B}_\varepsilon(\hat{\mathbf{x}}) \end{cases} , \tag{8}$$

$$\delta_\varepsilon := \begin{cases} 1 \text{ if } \mathbf{x} \in \Omega \setminus \overline{\mathcal{B}_\varepsilon(\hat{\mathbf{x}})} \\ \delta \text{ if } \mathbf{x} \in \mathcal{B}_\varepsilon(\hat{\mathbf{x}}) \end{cases} . \tag{9}$$

In addition, in (7) the function u_ε is solution of the following variational problem: find the temperature field $u_\varepsilon \in \mathcal{U}(\Omega_\varepsilon)$, such that

$$\int_{\Omega_\varepsilon} \gamma_\varepsilon \mathbf{K}\nabla u_\varepsilon \cdot \nabla \eta_\varepsilon - \int_{\Omega_\varepsilon} \delta_\varepsilon b\, \eta_\varepsilon + \int_{\Gamma_N} \bar{q}\eta_\varepsilon = 0 \quad \forall \eta_\varepsilon \in \mathcal{V}(\Omega_\varepsilon) \,, \tag{10}$$

and the set $\mathcal{U}(\Omega_\varepsilon)$ and the space $\mathcal{V}(\Omega_\varepsilon)$ are defined as

$$\mathcal{U}(\Omega_\varepsilon) := \left\{u_\varepsilon \in H^1(\Omega_\varepsilon) : u_\varepsilon|_{\Gamma_D} = \bar{u}\right\}, \tag{11}$$

$$\mathcal{V}(\Omega_\varepsilon) := \left\{\eta_\varepsilon \in H^1(\Omega_\varepsilon) : \eta_\varepsilon|_{\Gamma_D} = 0\right\}. \tag{12}$$

Finally, the Euler-Lagrange equation associated to variational problem (10) reads: find field u_ε, such that

$$\begin{cases} -\text{div}\,(\gamma_\varepsilon \mathbf{K}\nabla u_\varepsilon) = \delta_\varepsilon b \ \text{ in } \ \Omega_\varepsilon \\ u_\varepsilon = \bar{u} \quad \text{on } \Gamma_D \\ -\mathbf{K}\nabla u_\varepsilon \cdot \mathbf{n} = \bar{q} \quad \text{on } \Gamma_N \\ [\![u_\varepsilon]\!] = 0 \quad \text{on } \partial\mathcal{B}_\varepsilon \\ -[\![\gamma_\varepsilon \mathbf{K}\nabla u_\varepsilon]\!] \cdot \mathbf{n} = 0 \quad \text{on } \partial\mathcal{B}_\varepsilon \end{cases} . \tag{13}$$

In the above expression, we use $[\![(\cdot)]\!]$ to denotes the *jump* of function $(\cdot)$ across the boundary $\partial\mathcal{B}_\varepsilon$:

$$[\![(\cdot)]\!] := (\cdot)|_m - (\cdot)|_i \,, \tag{14}$$

with subscripts m and i associated, respectively, with quantity values on the matrix $(\Omega \setminus \overline{\mathcal{B}_\varepsilon(\hat{\mathbf{x}})})$ and inclusion $(\mathcal{B}_\varepsilon(\hat{\mathbf{x}}))$ sides of the interface.

3 Topological sensitivity analysis

Let us state the following result, leading to a constructive method for computing the topological derivatives, Sokołowski and Żochowski (2001), Novotny et al. (2003):

$$D_T\left(\hat{\mathbf{x}}\right) = \lim_{\varepsilon\to 0} \frac{1}{f'(\varepsilon)} \frac{d}{d\varepsilon} \mathcal{J}_{\Omega_\varepsilon}(u_\varepsilon) \,, \tag{15}$$

where $f'(\varepsilon)$ is the derivative of the function $f(\varepsilon)$ with respect to the parameter ε and the derivative of the perturbed cost functional $\frac{d}{d\varepsilon}\mathcal{J}_{\Omega_\varepsilon}(u_\varepsilon)$ may be seen as the classical sensitivity analysis to the change in shape produced by an uniform expansion of the inclusion.

In fact, considering a direct analogy with the continuum mechanics, see Gurtin (1981), we have that the shape derivative of the cost function $\mathcal{J}_{\Omega_\varepsilon}(u_\varepsilon)$ can be written as

$$\frac{d}{d\varepsilon}\mathcal{J}_{\Omega_\varepsilon}(u_\varepsilon) = \int_{\Omega_\varepsilon} \Sigma_\varepsilon \cdot \nabla \mathbf{v} \,, \tag{16}$$

where $\mathbf{v}$ is the *shape change velocity field* and tensor Σ_ε can be interpreted as a generalization of the Eshelby energy-momentum tensor, see Eshelby (1975) and Gurtin (2000), which is given in our particular case by

$$\Sigma_\varepsilon = \frac{1}{2}\left(\gamma_\varepsilon \mathbf{K}\nabla u_\varepsilon \cdot \nabla u_\varepsilon - 2\delta_\varepsilon b\, u_\varepsilon\right)\mathbf{I} - \gamma_\varepsilon \mathbf{K}\nabla u_\varepsilon \otimes \nabla u_\varepsilon \,. \tag{17}$$

Since u_ε is solution of the state equation (13), it is straightforward to verify that, in this particular case, the Eshelby tensor $\boldsymbol{\Sigma}_\varepsilon$ is a divergence-free field, i.e., $\text{div}\boldsymbol{\Sigma}_\varepsilon = \mathbf{0}$ in Ω_ε. Integrating (16) by parts and applying the divergence theorem, the shape derivative of the cost function $\mathcal{J}_{\Omega_\varepsilon}(u_\varepsilon)$ becomes an integral defined on the boundaries $\partial\Omega$ and $\partial\mathcal{B}_\varepsilon$, that is

$$\frac{d}{d\varepsilon}\mathcal{J}_{\Omega_\varepsilon}(u_\varepsilon) = \int_{\partial\Omega} \boldsymbol{\Sigma}_\varepsilon \mathbf{n}\cdot\mathbf{v} + \int_{\partial\mathcal{B}_\varepsilon} [\![\Sigma_\varepsilon]\!]\mathbf{n}\cdot\mathbf{v}\,, \tag{18}$$

where the normal vector field satisfies $\mathbf{n} := \mathbf{n}|_m = -\mathbf{n}|_i$ on $\partial\mathcal{B}_\varepsilon$. As a consequence, since the velocity field $\mathbf{v}$ is smooth enough in the domain Ω_ε, then the shape sensitivity of the problem only depends on the definition of this field on the boundaries $\partial\Omega$ and $\partial\mathcal{B}_\varepsilon$. However, in our particular case, we observe that only the boundary of the inclusion $\partial\mathcal{B}_\varepsilon$, is submitted to a perturbation (an uniform expansion). Therefore, remembering that $\mathbf{n}$ is the outward normal unit vector (see Fig. 1), the *velocity* $\mathbf{v}$ assumes the following values on the boundaries $\partial\mathcal{B}_\varepsilon$ and $\partial\Omega$

$$\begin{cases} \mathbf{v} = -\mathbf{n} & \text{on } \partial\mathcal{B}_\varepsilon \\ \mathbf{v} = \mathbf{0} & \text{on } \partial\Omega \end{cases}. \tag{19}$$

From this last remark and result (15), the topological derivative becomes an integral only defined on the boundary of the circular inclusion $\partial\mathcal{B}_\varepsilon$, that is

$$D_T(\widehat{\mathbf{x}}) = -\lim_{\varepsilon\to 0}\frac{1}{f'(\varepsilon)}\int_{\partial\mathcal{B}_\varepsilon} [\![\Sigma_\varepsilon]\!]\mathbf{n}\cdot\mathbf{n}\,. \tag{20}$$

3.1 Asymptotic analysis

The problem given by (13), even though linear, it is not so easy to expand in power of ε. Initially, consider a local coordinate system centered at $\widehat{\mathbf{x}}$ and oriented along the eigenvectors of tensor $\mathbf{K}$. Therefore, let us make the following change of variables

$$x_i = \sqrt{k_i}\, y_i \quad \text{for} \quad i = 1,2 \quad \Rightarrow \quad \mathbf{x} = \mathbf{K}^{\frac{1}{2}}\mathbf{y}, \tag{21}$$

where $\mathbf{x} = (x_1, x_2)$ and $\mathbf{y} = (y_1, y_2)$ are points defined over the domain Ω_ε and transformed domain $\tilde{\Omega}_\varepsilon$, respectively. Thus, the circular inclusion $\mathcal{B}_\varepsilon(\hat{\mathbf{x}})$ is mapped into an ellipse $\tilde{\mathcal{B}}_\varepsilon(\widehat{\mathbf{y}}) = \mathcal{E}_\varepsilon(\widehat{\mathbf{y}})$ with semi-major axis $\alpha = 1/\sqrt{k_1}$, semi-minor axis $\beta = 1/\sqrt{k_2}$ and centered at point $\widehat{\mathbf{y}}$, as can be seen in Fig. 3. The above mapping allows us to rewrite the Euler–Lagrange equation (13) as

$$\begin{cases} -\text{div}\,(\gamma_\varepsilon\nabla u_\varepsilon) = \delta_\varepsilon b & \text{in } \tilde{\Omega}_\varepsilon \\ u_\varepsilon = \bar{u} & \text{on } \tilde{\Gamma}_D \\ -\frac{\partial u_\varepsilon}{\partial n} = \bar{q} & \text{on } \tilde{\Gamma}_N \\ [\![u_\varepsilon]\!] = 0 & \text{on } \partial\tilde{\mathcal{B}}_\varepsilon \\ -[\![\gamma_\varepsilon\frac{\partial u_\varepsilon}{\partial n}]\!] = 0 & \text{on } \partial\tilde{\mathcal{B}}_\varepsilon \end{cases}, \tag{22}$$

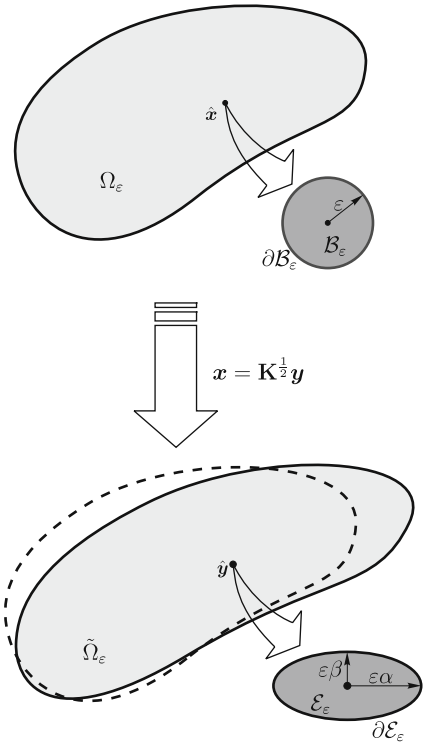

Fig. 3 Change of variables

where for the sake of simplicity we are using the same notation for field u_ε, heat source b and boundary conditions $\bar{q}$ and $\bar{u}$. Then, the following asymptotic expansion of solution $u_\varepsilon(\mathbf{y})$ in $\tilde{\Omega}_\varepsilon$ holds (Cedio-Fengya et al. 1998; Brühl 2003; Ammari and Kang 2004; Nazarov and Sokołowski 2006),

$$u_\varepsilon(\mathbf{y})\big|_{\tilde{\Omega}\setminus\overline{\mathcal{E}_\varepsilon(\hat{\mathbf{y}})}} = u(\mathbf{y}) + \frac{\varepsilon}{\|\boldsymbol{\zeta}\|^2}\mathbf{P}\nabla u(\widehat{\mathbf{y}})\cdot\boldsymbol{\zeta} + \mathcal{O}(\varepsilon^2), \tag{23}$$

$$u_\varepsilon(\mathbf{y})\big|_{\mathcal{E}_\varepsilon(\hat{\mathbf{y}})} = u(\mathbf{y}) + \varepsilon\mathbf{P}\nabla u(\widehat{\mathbf{y}})\cdot\boldsymbol{\zeta} + \mathcal{O}(\varepsilon^2), \tag{24}$$

where $\boldsymbol{\zeta} = (\mathbf{y} - \widehat{\mathbf{y}})/\varepsilon$, $u(\mathbf{y})$ is the solution of the problem in the unperturbed domain $\tilde{\Omega}$, $\nabla u(\widehat{\mathbf{y}})$ is the corresponding gradient evaluated at point $\widehat{\mathbf{y}}$ (the centre of the ellipse) and $\mathbf{P}$ is given by

$$\mathbf{P} = \frac{1}{2}(1-\gamma)\alpha\beta\begin{pmatrix} \frac{\alpha+\beta}{\alpha+\gamma\beta} & 0 \\ 0 & \frac{\alpha+\beta}{\beta+\gamma\alpha} \end{pmatrix}, \tag{25}$$

which has been derivated from the polarization tensor for an elliptical inclusion, Pólya and Szegö (1951).

Considering the inverse mapping $\mathbf{y} = \mathbf{J}\mathbf{x}$ in (23, 24), where $\mathbf{J} := \mathbf{K}^{-\frac{1}{2}}$, we have that the asymptotic expansion for $u_\varepsilon(\mathbf{x})$ in Ω_ε is given by

$$u_\varepsilon(\mathbf{x})|_{\Omega\setminus\overline{\mathcal{B}_\varepsilon(\hat{\mathbf{x}})}} = u(\mathbf{x}) + \frac{\varepsilon}{\|\mathbf{J}\boldsymbol{\xi}\|^2}\mathbf{P}\nabla u(\widehat{\mathbf{x}})\cdot\boldsymbol{\xi} + \mathcal{O}(\varepsilon^2), \tag{26}$$

$$u_\varepsilon(\mathbf{x})|_{\mathcal{B}_\varepsilon(\hat{\mathbf{x}})} = u(\mathbf{x}) + \varepsilon\mathbf{P}\nabla u(\widehat{\mathbf{x}})\cdot\boldsymbol{\xi} + \mathcal{O}(\varepsilon^2), \tag{27}$$

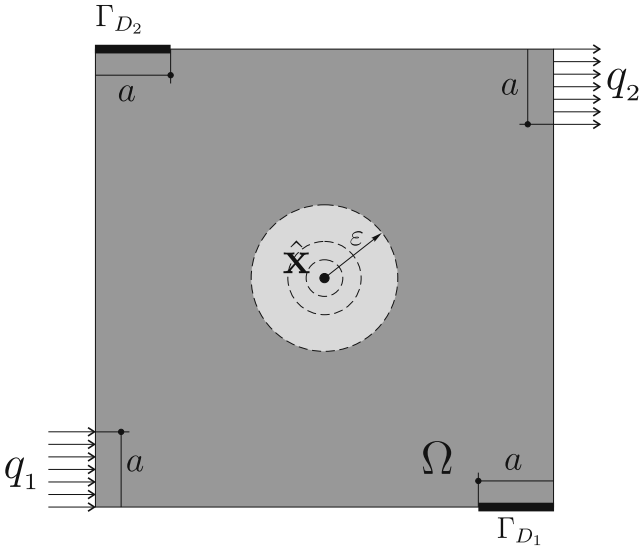

(a) Domain.

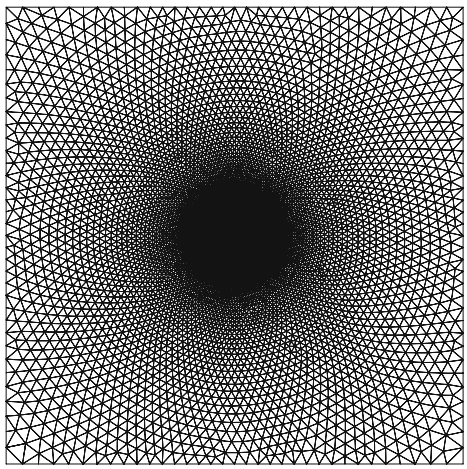

(b) Finite element mesh.

Fig. 4 Numerical verification. Domain and finite elements mesh (**a**, **b**)

where $\boldsymbol{\xi} = (\mathbf{x} - \widehat{\mathbf{x}})/\varepsilon$. It is well known that the asymptotic expansions can be differentiated term by term (Maz'ya et al. 1981; Mazja et al. 1991). Thus, by assuming a sufficient regularity of $u(\mathbf{x})$ in Ω and performing its Taylor series expansion around point $\widehat{\mathbf{x}}$, we obtain the following expansion for $\nabla u_\varepsilon(\mathbf{x})$ in Ω_ε,

$$\nabla u_\varepsilon(\mathbf{x})|_{\Omega \setminus \overline{\mathcal{B}_\varepsilon(\widehat{\mathbf{x}})}} = \nabla u(\widehat{\mathbf{x}}) + \frac{1}{\|\mathbf{J}\boldsymbol{\xi}\|^2}\mathbf{SP}\nabla u(\widehat{\mathbf{x}}) + \mathcal{O}(\varepsilon), \quad (28)$$

$$\nabla u_\varepsilon(\mathbf{x})|_{\mathcal{B}_\varepsilon(\widehat{\mathbf{x}})} = \nabla u(\widehat{\mathbf{x}}) + \mathbf{P}\nabla u(\widehat{\mathbf{x}}) + \mathcal{O}(\varepsilon), \quad (29)$$

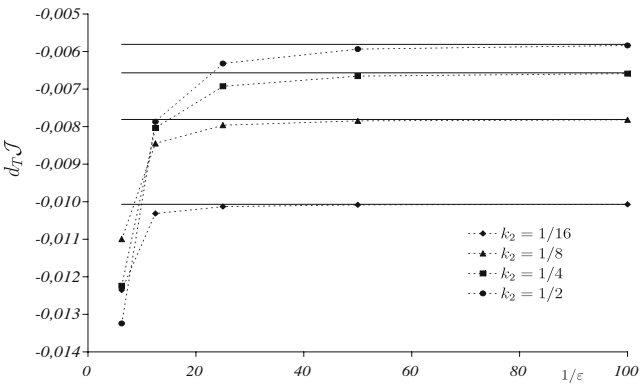

(a) $k_1 = 1$ and $k_2 < 1$.

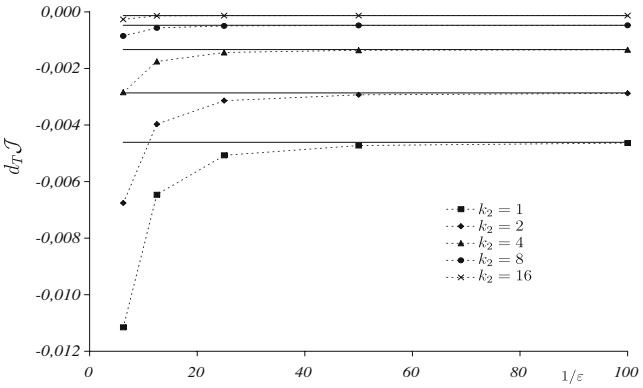

(b) $k_1 = 1$ and $k_2 \geq 1$.

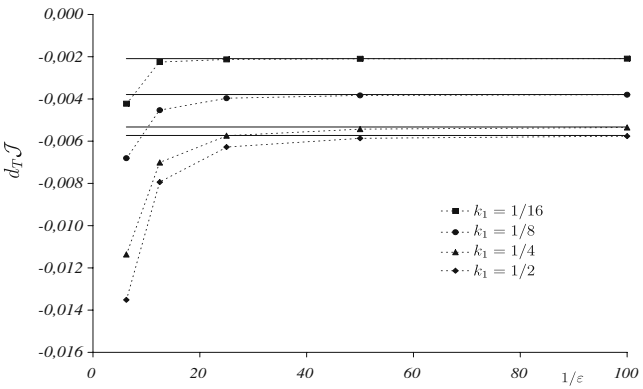

(c) $k_2 = 1$ and $k_1 < 1$.

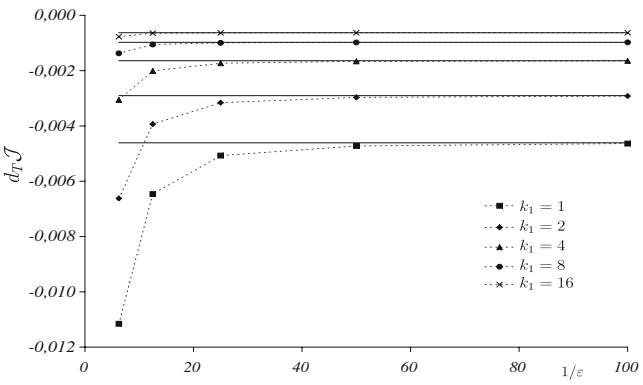

(d) $k_2 = 1$ and $k_1 \geq 1$.

Fig. 5 Numerical verification. Convergence of numerical topological derivative to analytical value for $\gamma = 1/2$ (**a**–**d**)

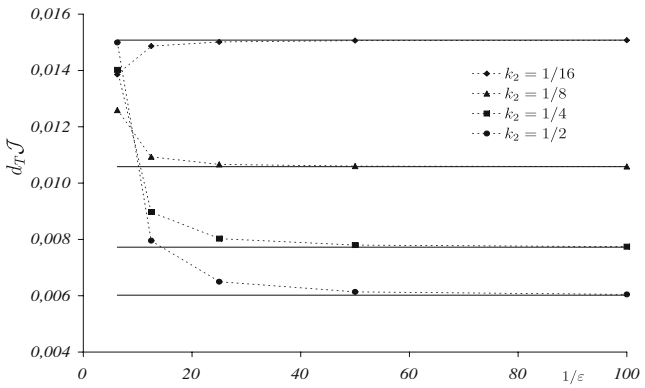

(a) $k_1 = 1$ and $k_2 < 1$.

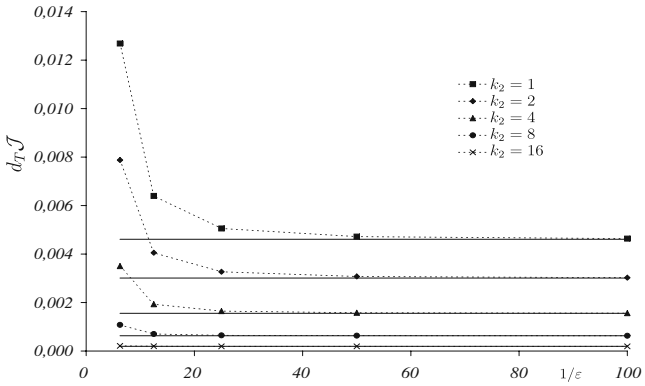

(b) $k_1 = 1$ and $k_2 \geq 1$.

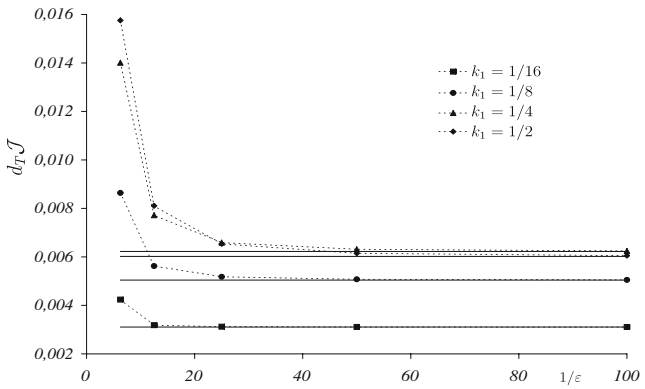

(c) $k_2 = 1$ and $k_1 < 1$.

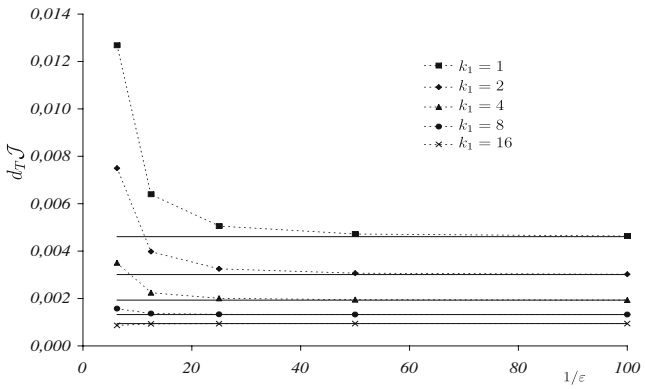

(d) $k_2 = 1$ and $k_1 \geq 1$.

◀ **Fig. 6** Numerical verification. Convergence of numerical topological derivative to analytical value for $\gamma = 2$ (**a**–**d**)

with

$$\mathbf{S} := \mathbf{I} - \frac{2}{\|\mathbf{J}\boldsymbol{\xi}\|^2}\mathbf{J}^2\boldsymbol{\xi} \otimes \boldsymbol{\xi} \ . \tag{30}$$

3.2 Topological derivative calculation

From expansions (26–29), and using symbolic calculus to solve the integral (20) (choosing the function $f(\varepsilon)$ as the size of the perturbation, i.e., $f(\varepsilon) = \pi\varepsilon^2$) we have that the final expression of the topological derivative becomes a scalar function that depends on the solution u associated to the original domain Ω (without inclusion), that is (see also Amstutz 2006):

$$D_T(\widehat{\mathbf{x}}) = -\sqrt{\det \mathbf{K}}\,\mathbf{K}\mathbf{P}\nabla u(\widehat{\mathbf{x}}) \cdot \nabla u(\widehat{\mathbf{x}}) + (1-\delta) b\, u(\widehat{\mathbf{x}}) \qquad \forall \widehat{\mathbf{x}} \in \Omega \ . \tag{31}$$

Remark 1 From the final expression of the topological derivative for the steady-state orthotropic heat diffusion problem (31), we can analyze the limits cases of the parameter γ, which are:

– ideal thermal insulator ($\gamma \to 0$):

$$D_T(\widehat{\mathbf{x}}) = -\frac{1}{2}\frac{\mathbf{K}}{\sqrt{\det \mathbf{K}}}\left(\sqrt{\det \mathbf{K}}\,\mathbf{I} + \mathbf{K}\right)\nabla u(\widehat{\mathbf{x}}) \cdot \nabla u(\widehat{\mathbf{x}}) + (1-\delta) b\, u(\widehat{\mathbf{x}}) \qquad \forall \widehat{\mathbf{x}} \in \Omega \ , \tag{32}$$

– ideal thermal conductor ($\gamma \to \infty$):

$$D_T(\widehat{\mathbf{x}}) = \frac{1}{2}\left(\sqrt{\det \mathbf{K}}\,\mathbf{I} + \mathbf{K}\right)\nabla u(\widehat{\mathbf{x}}) \cdot \nabla u(\widehat{\mathbf{x}}) + (1-\delta) b\, u(\widehat{\mathbf{x}}) \qquad \forall \widehat{\mathbf{x}} \in \Omega \ . \tag{33}$$

Remark 2 It is interesting to observe that for isotropic material, we have $k_1 = k_2 = k$ and the final expression for the topological derivative (31) degenerates to the classical one given by Amstutz (2006),

$$D_T(\widehat{\mathbf{x}}) = -k\frac{1-\gamma}{1+\gamma}\nabla u(\widehat{\mathbf{x}}) \cdot \nabla u(\widehat{\mathbf{x}}) + (1-\delta) b\, u(\widehat{\mathbf{x}}) \qquad \forall \widehat{\mathbf{x}} \in \Omega \ . \tag{34}$$

3.3 Numerical verification

In direct analogy with classical finite difference-based methods for the numerical approximation of the derivative of a generic function, a first order *topological finite difference* formula based on (2) to approximate

numerically the value of $D_T(\widehat{\mathbf{x}})$ at the unperturbed domain can be defined as

$$d_T\mathcal{J} := \frac{\mathcal{J}_{\Omega_\varepsilon}(u_\varepsilon) - \mathcal{J}_\Omega(u)}{f(\varepsilon)}\,, \tag{35}$$

with finite ε. The above satisfies

$$\lim_{\varepsilon\to 0} d_T\mathcal{J} = D_T(\widehat{\mathbf{x}})\,. \tag{36}$$

If for a given domain we calculate $\mathcal{J}_\Omega(u)$ and its perturbed counterpart $\mathcal{J}_{\Omega_\varepsilon}(u_\varepsilon)$ for a sequence of decreasing (sufficiently small) inclusion radii ε, the use of formula (35) will provide an asymptotic approximation to the analytical value of $D_T(\widehat{\mathbf{x}})$ given by (31). Here such a procedure is used to provide a numerical validation of result (31). The required values of function $\mathcal{J}_\Omega$ and $\mathcal{J}_{\Omega_\varepsilon}$ are computed numerically by means of the standard Finite Element Method for steady-state orthotropic heat diffusion problems.

For this instance, we have a unit square body without heat source ($b = 0$) and submitted to a temperature $\bar{u} = 0$ on Γ_{D_1} and Γ_{D_2}, a heat flux $q_1 = 1.0$ on Γ_{N_1} and $q_2 = 2.0$ on Γ_{N_2}, as shown in Fig. 4a, where $a = 0.2$. In addition, the remainder part of the boundary remains insulated. For the computation of the values of $\mathcal{J}_{\Omega_\varepsilon}(u_\varepsilon)$, a sequence of finite element analyses are carried out for perturbed domains obtained by introducing circular inclusions of radii

$$\varepsilon \in \{0.16, 0.08, 0.04, 0.02, 0.01\}, \tag{37}$$

centred at $\hat{\mathbf{x}} = (0.5, 0.5)$. The finite element mesh used to discretise the domain Ω_ε was built so that each boundary of radius ε has 120 six-noded (quadratic) triangular isoparametric elements. The obtained mesh contains 50781 nodes and 25322 elements, as can be see in Fig. 4b.

For this numerical verification two cases for the parameter γ are studied: *(i)* $\gamma = 1/2$; and *(ii)* $\gamma = 2$.

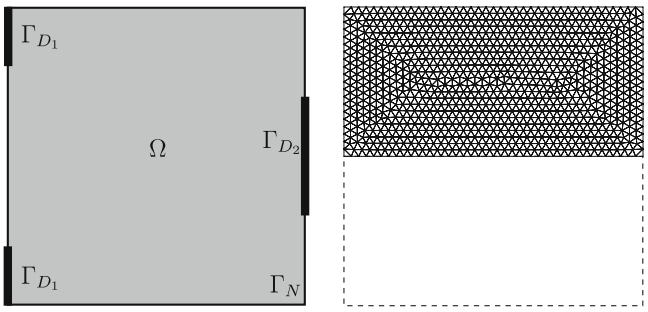

(a) Domain. (b) Mesh.

Fig. 7 Example 1, Experiment 1. Domain and finite elements mesh (**a**, **b**)

The results of the analyses are plotted in Fig. 5 and Fig. 6, respectively, which shows the analytical topological derivative and the numerical approximations for each value of ε for values of parameters k_1 and k_2 between 1/16 and 16.

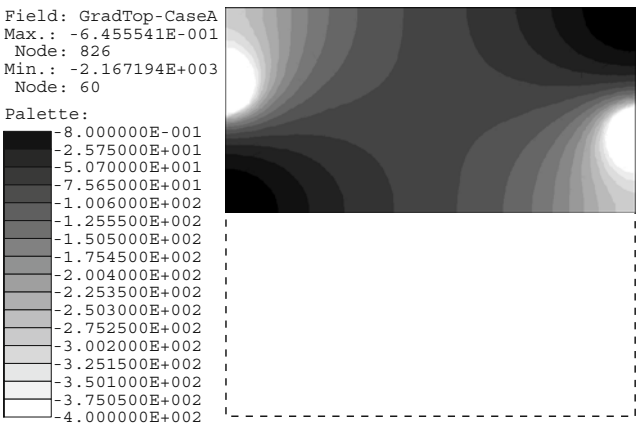

(a) Case A.

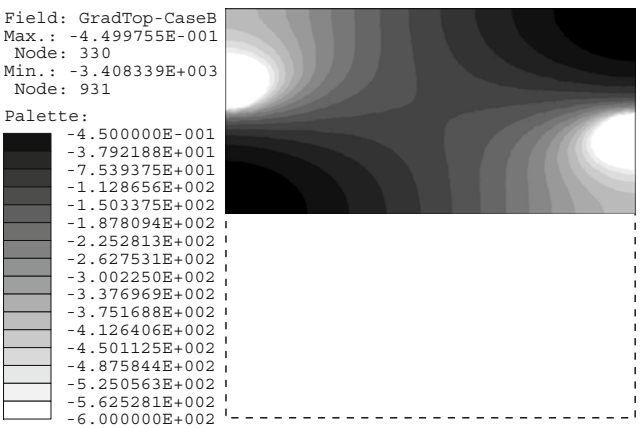

(b) Case B.

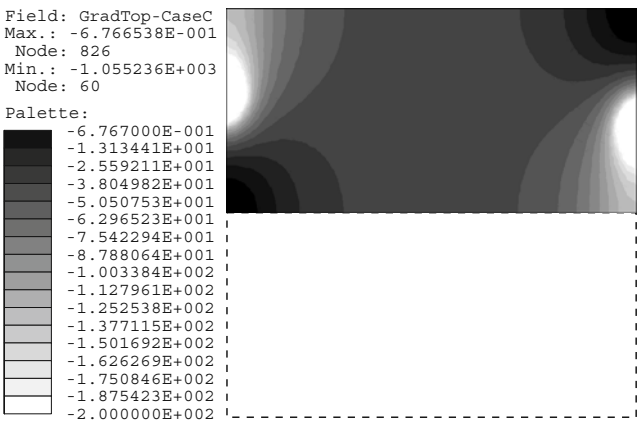

(c) Case C.

Fig. 8 Example 1, Experiment 1. Topological derivative value for $\gamma \to 0$ (**a**–**c**)

The convergence of the numerical topological derivatives to their corresponding analytical values with decreasing ε is obvious in all cases and confirm the correctness of formula (31).

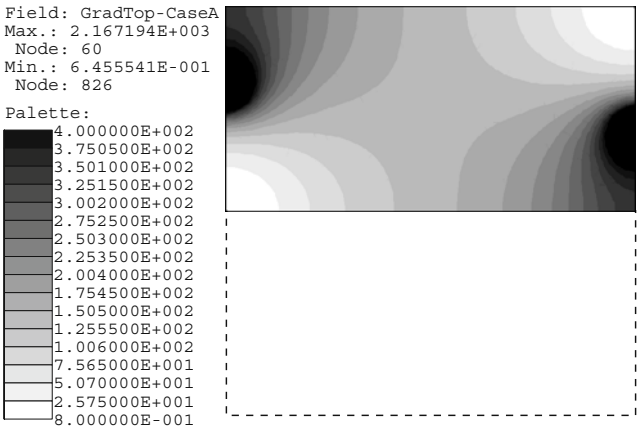

(a) Case A.

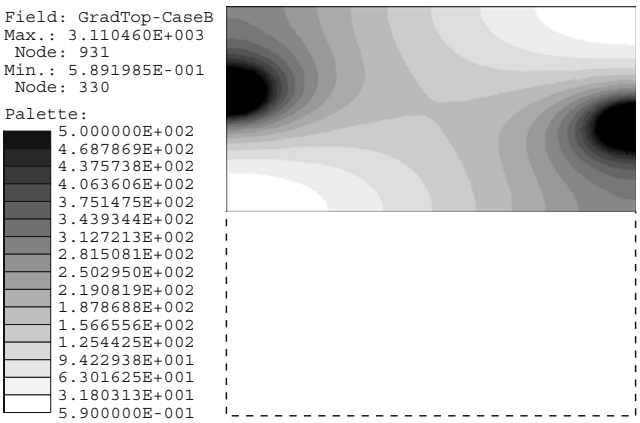

(b) Case B.

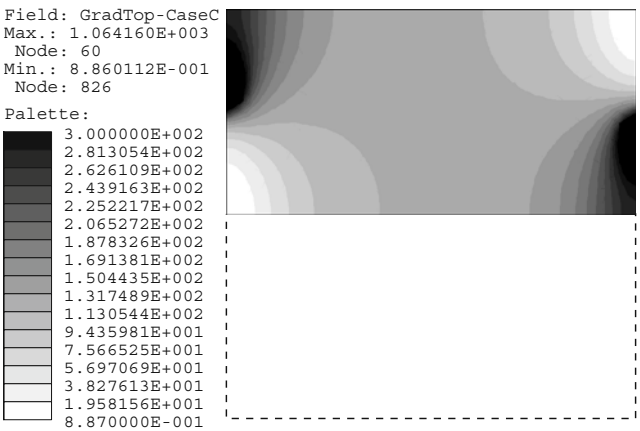

(c) Case C.

Fig. 9 Example 1, Experiment 1. Topological derivative value for $\gamma \to \infty$ (**a**–**c**)

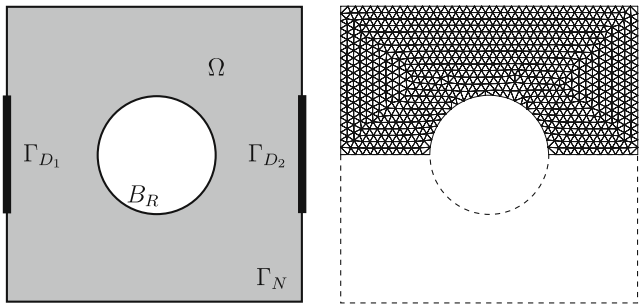

(a) Domain. (b) Mesh.

Fig. 10 Example 1, Experiment 2. Domain and finite elements mesh (**a**, **b**)

4 Numerical examples

In this section we present two examples considering different values of the orthotropic thermal conductivities parameters k_1 and k_2, namely:

- **Case A:** $k_1 = k_2 = 2$ (isotropic behavior),
- **Case B:** $k_1 = 3$ and $k_2 = 1$,
- **Case C:** $k_1 = 1$ and $k_2 = 3$.

The first one concerns two numerical experiments showing the behavior of the topological sensitivity field taking into account the limit cases $\gamma \to 0$ and $\gamma \to \infty$. In the second example, the topological derivative is used in the optimal design of heat conductors. In all examples we consider a set $\mathcal{D} = (0, 10) \times (0, 10)$ such that the domain $\Omega \subseteq \mathcal{D}$, whose boundary is given by $\partial\Omega = \Gamma_D \cup \Gamma_N$ with $\Gamma_N \cap \Gamma_D = \varnothing$.

4.1 Example 1

For this example we consider a domain Ω without heat source ($b = 0$) and the Dirichlet boundary Γ_D is such that: $\Gamma_D = \Gamma_{D_1} \cup \Gamma_{D_2}$ with $meas(\Gamma_{D_1}) = meas(\Gamma_{D_2}) = 4$. We study the behavior of the limits cases given by (32) and (33).

Experiment 1 In this first experiment $\Omega = \mathcal{D}$ and the boundary condition are given by: on Γ_N we have that $\bar{q} = 0$ and on Γ_{D_1} and Γ_{D_2} are prescribed the temperatures $\bar{u}_1 = 0$ and $\bar{u}_2 = 100$, respectively. Due to the symmetry of the problem, only half of the domain is discretized. For discretization we use an uniform mesh with 1822 tree-noded (linear) triangular elements with a total of 972 nodes. The domain Ω and the finite element mesh are shown in Fig. 7a and 7b, respectively.

The topological derivative field obtained for the ideal thermal insulator case ($\gamma \to 0$) is shown in Fig. 8 and, for the ideal thermal conductor case ($\gamma \to \infty$) in Fig. 9.

Experiment 2 In Fig. 10a we show the disposition of boundaries Γ_{D_1}, Γ_{D_2}, Γ_N and the domain $\Omega = \mathcal{D}\backslash\overline{B_R}$, where B_R denote a ball with radius $R = 2.0$ and centered at point $\mathbf{x} = (5.0, 5.0)$. In this case, the boundary conditions are the same that for the previous experiment. Due to the symmetry of the problem, only half of the domain is discretized. For discretization we use an uniform mesh with 1583 tree-noded (linear) triangular elements with a total of 857 nodes. In Fig. 10b is shown the finite element mesh used in this experiment.

In Fig. 11 is shown the topological derivative field for the ideal thermal insulator case ($\gamma \to 0$) and in Fig. 12 for the ideal thermal conductor case ($\gamma \to \infty$).

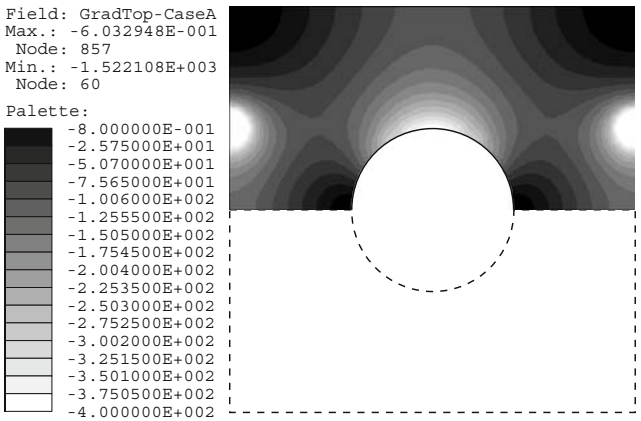

(a) Case A.

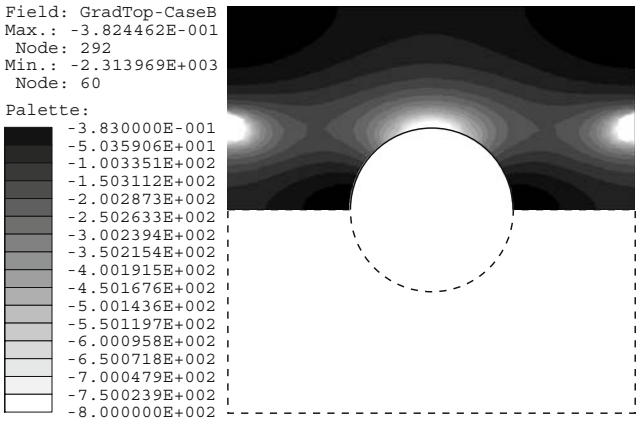

(b) Case B.

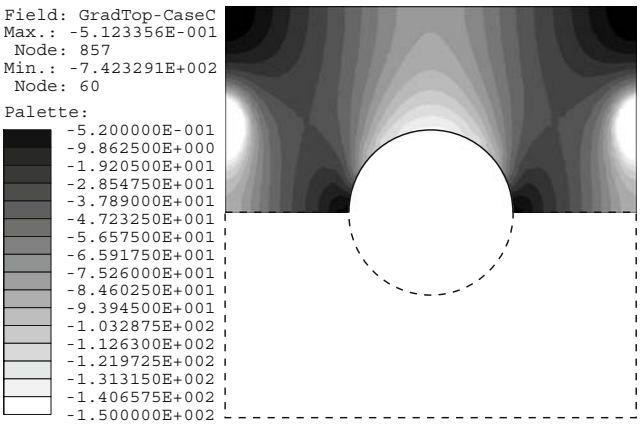

(c) Case C.

Fig. 11 Example 1, Experiment 2. Topological derivative value for $\gamma \to 0$ (**a**–**c**)

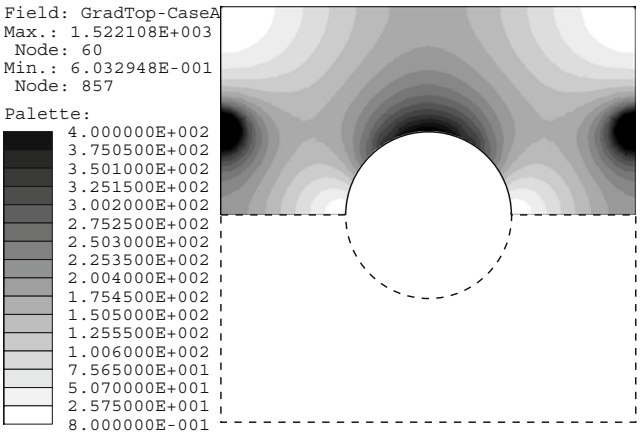

(a) Case A.

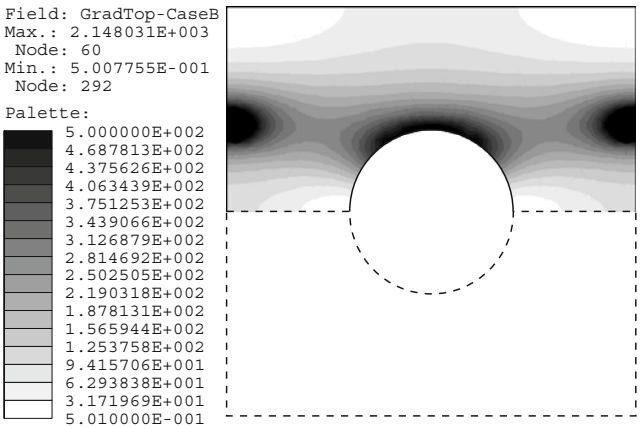

(b) Case B.

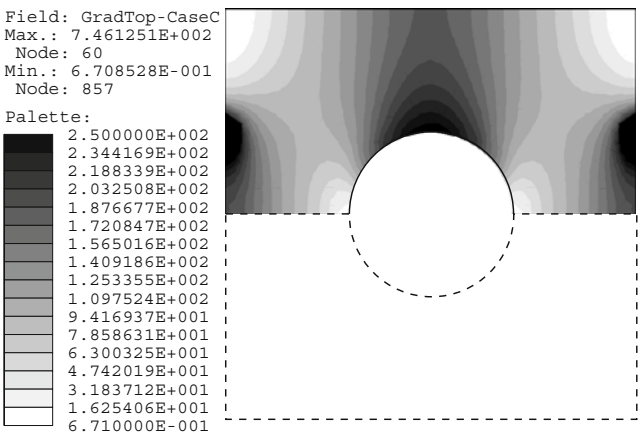

(c) Case C.

Fig. 12 Example 1, Experiment 2. Topological derivative value for $\gamma \to \infty$ (**a**–**c**)

These experiments, although academic, shows that the topological derivative can be used to determine where the holes (or inclusion) must be positioned (points $\widehat{\mathbf{x}}$ in which $D_T(\widehat{\mathbf{x}})$ assumes the value closer to zero) in order to minimize (or maximize) the shape functional, in this case, the total potential energy associated to the steady-state orthotropic heat diffusion problem. In particular, in both examples the region in which the topological derivative assume the value closer to zero is almost the same for the three cases. But in Case C this region is bigger than in the others two cases, due to, in part, to the fact that the direction of the heat flux corresponds with the direction of higher coefficient of the thermal conductivity tensor.

4.2 Example 2

In this second example we use the topological derivative field (31) to perform the optimal design of heat conductors. To this ends we use the topology optimization algorithm developed in Giusti et al. (2008). In Fig. 14a is presented the design domain $\Omega = \mathcal{D}$, whose boundary remain isolated except for a region Γ_D of size $meas(\Gamma_D) = 2$, positioned in the middle of the left side in which the temperature is prescribed as $\bar{u} = 0$. We also consider an uniform heat generation $b = 1$ over all the domain Ω ($\delta = 1$). For this example, we have two materials: a good conductor characterized by the thermal conductivities previously mentioned (Case A, B or C) and a bad conductor (or insulator) characterized by the parameter $\gamma = 0.001$. For all cases, the initial configuration is the previously described domain (shown in Fig. 14a) composed by 100% of good thermal conductor. Finally, the volume constraint is chosen to be 40% of good conductor material. Due to the symmetry of the problem, only half of the domain is discretized. For discretization we use an uniform mesh with 46212 tree-noded (linear) triangular elements with a total of 23407 nodes.

The value of the shape functional $\psi(\Omega_\varepsilon)$ throughout the optimization procedure previously referred is presented in Fig. 13. In Fig. 14 we shown the obtained topologies for the three studied cases for the different

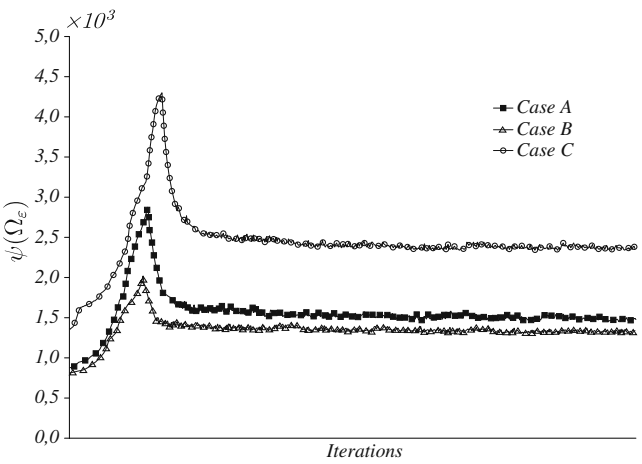

Fig. 13 Example 2. Total potential energy

Fig. 14 Example 2. Model and obtained topologies (**a**–**d**)

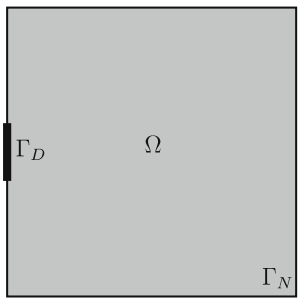

(a) Model.

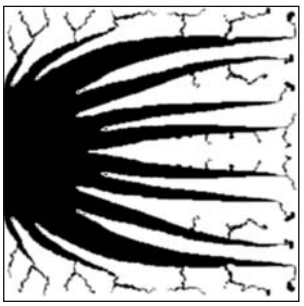

(b) Case A.

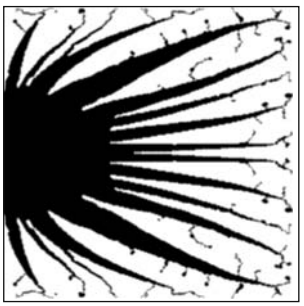

(c) Case B.

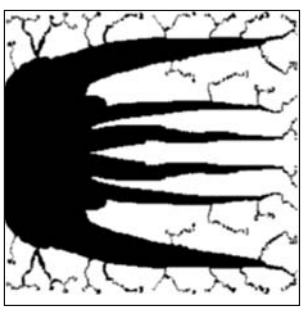

(d) Case C.

values of the thermal conductivities. In the figures, the black material represents the good thermal conductor.

In this final example, we show how the topological derivative field can be used in the topological design of heat conductors. As expected, the obtained result, Fig. 14, show how the good conductor drains energy from all parts of the domain. Similar results, for the isotropic case, can be found in the literature, see Bendsøe and Sigmund (2003) for instance.

5 Final remarks

An analytical expression for the topological derivative associated to the total potential energy in steady-state orthotropic heat diffusion problem, when a circular inclusion of the same nature as the bulk material is introduced at an arbitrary point of the domain, has been proposed in this paper. The final formula was obtained using a simple changing of variable and the first order Pólya-Szegö polarization tensor. Thus, besides to extend the result presented in Sokołowski and Żochowski (1999), we have shown that the approach here adopted (Novotny et al. 2003) can be in fact applied to arbitrary shaped holes or inclusions (an elliptical inclusion in this case), contrary to the comment by Amstutz and Dominguez (2008). In order to verify the proposed analytical expression, we have developed a numerical validation showing the convergence of the numerical topological derivative to their corresponding analytical value. The obtained result was used to devise two numerical examples. The first one shows the behavior of the topological derivative field for different values of the orthotropic thermal conductivity. For the second numerical example, the topological derivative formula is used in the design of heat conductors. Finally, we remark that this information can be potentially used, as shown in the numerical examples, in a number of applications of practical interest such as, for instance: image restoration algorithm, optimization of mechanical or electronic pieces, design of an orthotropic material to achieve a specified thermal behavior.

Acknowledgements This research was financially supported by Brazil/France program CAPES/COFECUB under the grant 604/08. S.M. Giusti was supported by CAPES (Brazilian Higher Education Staff Training Agency). This support is gratefully acknowledged.

References

Allaire G, Gournay F, Jouve F, Toader A (2005) Structural optimization using topological and shape sensitivity via a level set method. Control Cybern 34(1):59–80

Ammari H, Kang H (2004) Reconstruction of small inhomogeneities from boundary measurements. Lectures Notes in Mathematics, vol 1846. Springer, Berlin

Amstutz S (2006) Sensitivity analysis with respect to a local perturbation of the material property. Asymptot Anal 49 (1–2):87–108

Amstutz S, Andrä H (2006) A new algorithm for topology optimization using a level-set method. J Comput Phys 216(2):573–588

Amstutz S, Dominguez N (2008) Topological sensitivity analysis in the context of ultrasonic non-destructive testing. Eng Anal Bound Elem 32(11):936–947

Amstutz S, Horchani I, Masmoudi M (2005) Crack detection by the topological gradient method. Control Cybern 34(1): 81–101

Auroux D, Masmoudi M, Belaid L (2007) Image restoration and classification by topological asymptotic expansion. In: Variational formulations in mechanics: theory and applications. Barcelona

Bendsøe MP, Sigmund O (2003) Topology optimization. Theory, methods and applications. Springer, Berlin

Bonnet M (2006) Topological sensitivity for 3d elastodynamic and acoustic inverse scattering in the time domain. Comput Methods Appl Mech Eng 195(37–40):5239–5254

Brühl M, Hanke M, Vogelius MS (2003) A direct impedance tomography algorithm for locating small inhomogeneities. Numer Math 93:635–654

Céa J, Garreau S, Guillaume P, Masmoudi M (2000) The shape and topological optimizations connection. Comput Methods Appl Mech Eng 188(4):713–726

Cedio-Fengya D, Moskow S, Vogeliu M (1998) Identification of conductivity imperfections of small diameter by boundary measurements. Continuous dependence and computational reconstruction. Inverse Probl 14(3):553–595

Eschenauer H, Kobelev V, Schumacher A (1994) Buble method for topology and shape optmization of structures. Struct Optim 8(1):42–51

Eshelby J (1975) The elastic energy-momentum tensor. J Elast 5(3–4):321–335

Feijóo G (2004) A new method in inverse scattering based on the topological derivative. Inverse Probl 20(6):1819–1840

Fulmanski P, Lauraine A, Scheid J, Sokołowski J (2007) A level set method in shape and topology optimization for variational inequalities. Int J Appl Math Comput Sci 17(3): 413–430

Fulmanski P, Lauraine A, Scheid J, Sokołowski J (2008) A level set method in shape and topology optimization for variational inequalities. Int J Comput Math 85(10):1491–1514

Giusti S, Novotny A, Padra C (2008) Topological sensitivity analysis of inclusion in two-dimensional linear elasticity. Eng Anal Bound Elem 32(11):926–935

Gurtin M (1981) An introduction to continuum mechanics. Mathematics in Science and Engineering, vol 158. Academic, New York

Gurtin M (2000) Configurational forces as basic concept of continuum physics. Applied mathematical sciences, vol 137. Springer, New York

Hintermüller M (2005) Fast level set based algorithms usind shape and topological sensitivity. Control Cybern 34(1): 305–324

Larrabide I, Feijóo R, Novotny A, Taroco E (2008) Topological derivative: a tool for image processing. Comput Struct 86(13–14):1386–1403

Lee S, Kwak B (2008) Smooth boundary topology optimization for eigenvalue performance and its application to the design of a flexural stage. Eng Optim 40(3):271–285

Mazja W, Nasarow S, Plamenewski B (1991) Asymptotische Theorie elliptischer Randwertaufgaben in singulär gestörten Gebieten, vol 1 (English translation: asymptotic theory of elliptic boundary value problems in singularly perturbed domains, vol 1, Basel: Birkhäuser Verlag, 2000). Akademie, Berlin

Maz'ya V, Nazarov S, Plamenewski B (1981) Asymptotics of solutions to elliptic boundary-value problems under a singular perturbation of the domain (Russian). Tbilisi University, Tbilisi

Nazarov S, Sokołowski J (2003) Asymptotic analysis of shape functionals. J Math Pures Appl 82(2):125–196

Nazarov S, Sokołowski J (2006) Self-adjoint extensions for the neumann laplacian and applications. Acta Math Appl Sin 22(3):879–906

Norato J, Bendsøe M, Haber R, Tortorelli D (2007) A topological derivative method for topology optimization. Struct Multidisc Optim 33(4–5):375–386

Novotny A, Feijóo R, Padra C, Taroco E (2003) Topological sensitivity analysis. Comput Methods Appl Mech Eng 192(7–8):803–829

Pólya G, Szegö G (1951) Izoperimetric inequalities in mathematical physics. Princeton University Press, Princeton

Sokołowski J, Żochowski A (1999) On the topological derivatives in shape optmization. SIAM J Control Optim 37(4): 1251–1272

Sokołowski J, Żochowski A (2001) Topological derivatives of shape functionals for elasticity systems. Mechan Struct Mach 29(3):333–351